Temperature structure functions in turbulent shear flows

R. A. Antonia
Department of Mechanical Engineering, University of Newcastle, New South Wales 2308, Australia

E. J. Hopfinger, Y. Gagne, and F. Anselmet
Institut de Mécanique, Université Scientifique et Médicale de Grenoble, F-38402, Saint Martin d'Hères Cédex, France
(Received 2 April 1984)

The inertial-range behavior of measured temperature structure functions, up to order 12, is compared with predictions by the log-normal and the β model. Both models are unsatisfactory from a quantitative viewpoint. The comparison between measurements and models indicates that the intermittency of the temperature field is different from that of the velocity field.

I. INTRODUCTION

In general, the nth-order longitudinal velocity structure function in a turbulent flow can be written as

$$\langle (\Delta u)^n \rangle = \langle [u(x+r)-u(x)]^n \rangle \sim \langle \epsilon \rangle^{n/3} r^{\alpha_n} \tag{1}$$

when the separation r lies within the inertial range $\eta \ll r \ll l$, the lower and upper limits being usually identifiable with the Kolmogorov length scale $\nu^{3/4}\langle \epsilon \rangle^{-1/4}$ (ν is the kinematic viscosity of the fluid, $\langle \epsilon \rangle$ is the average turbulent energy dissipation) and the turbulence integral length scale, respectively. For the log-normal model[1-3] the exponent α_n is given by (see, e.g., Ref. 4)

$$\alpha_n = \frac{n}{3} - \frac{\mu}{18} n(n-3) , \tag{2}$$

whilst for the β model, developed by Frisch *et al.*[5] and related to the Novikov-Stewart model,[6]

$$\alpha_n = \frac{n}{3} - \frac{\mu}{3}(n-3) . \tag{3}$$

The constant μ in (2) and (3) is the exponent in the following autocorrelation:

$$\langle \epsilon(x)\epsilon(x+r) \rangle \sim \left[\frac{l}{r} \right]^{\mu} . \tag{4}$$

Recent measurements (e.g., Refs. 7 and 8) have indicated a value of μ of about 0.2. With this value of μ large values of n are required to distinguish between the different behaviors reflected by (2) and (3). It is for this reason that Anselmet *et al.*[8] measured velocity structure functions in a turbulent circular jet of order as high as 18.

In the light of the previous remarks, it would seem reasonable to expect that, in the case of the temperature field, high-order moment temperature structure functions would be required to allow an unambiguous decision to be made about the suitability of different models. To this purpose we first briefly recall in Sec. II the results for the log-normal model and indicate the results for the β model, when the latter is used to account for the intermittency of the temperature field. The difficulty in obtaining reliable measurements of high-order temperature structure functions is briefly discussed in Sec. III. The measurements are then discussed in Sec. IV in the context of predictions by the two models.

II. THE LOG-NORMAL AND β MODELS

The log-normal model assumes a probabilistic knowledge of the dissipation rates. In the β model the attention is focused on the inertial transfer rate of ϵ_r for reasons given in Refs. 5 and 9. It is in this latter spirit that we develop the arguments for the temperature β model.

The transfer of turbulent energy ϵ_r from a volume of linear dimension r to smaller scales can be taken equal to $(\delta u)^2/\delta t$, where $\delta u(r)$ is the velocity difference and the time scale δt is given by the ratio $r/\delta u$. It follows that

$$\epsilon_r \sim \frac{(\delta u)^3}{r} , \tag{5}$$

where ϵ_r could also be thought of as the dissipation rate of turbulent energy. In an analogous manner, the transfer χ_r of temperature variance to smaller scales is given by the ratio $(\delta\theta)^2/\delta t$, where $\delta\theta(r)$ is the temperature difference over the volume of dimension r. It follows that

$$\chi_r \sim \frac{(\delta u)(\delta\theta)^2}{r} , \tag{6}$$

where χ_r could also be thought of as the dissipation rate of temperature variance. If δu and $\delta\theta$ are identified with the velocity Δu and temperature $\Delta\theta$ increments, respectively, products of these increments, of order $m+n$, will be given by

$$(\Delta u)^m (\Delta\theta)^n \sim r^{(m+n)/3} \epsilon_r^{m/3-n/6} \chi_r^{n/2} . \tag{7}$$

Before considering the average value of (7) we note that the effect of intermittency in χ_r is usually quantified through the power-law exponent μ_θ in a manner analogous to (4),

$$\langle \chi(x)\chi(x+r) \rangle \sim \left[\frac{l}{r} \right]^{\mu_\theta} . \tag{8}$$

In Ref. 5 it was conjectured that, for homogeneous turbulence, the sixth-order velocity structure function was directly related to the autocorrelation of ϵ, i.e.,

$$\langle (\Delta u)^6 \rangle \sim r^2 \langle \epsilon(x)\epsilon(x+r) \rangle \ . \tag{9}$$

It is not difficult to show that an analogous relation for temperature is

$$\langle (\Delta u)^2 \rangle (\Delta\theta)^4 \rangle \sim r^2 \langle \chi(x)\chi(x+r) \rangle \ . \tag{10}$$

Expressions (4), (8), (9), and (10) suggest that the exponents μ and μ_θ can be inferred from either dissipation correlation measurements or measurements of the structure functions. Both types of measurements indicated that $\mu \simeq 0.2$. A more recent evaluation[8] of available experimental data, while supporting this value of μ, indicates that appropriate upper and lower bounds of μ are 0.25 and 0.15, respectively. Measured autocorrelations[10] of individual components of χ indicated a value of 0.25 for μ_θ, the same value as predicted by Mori.[11] Atmospheric data[12] for $\langle (\Delta u)^2 (\Delta\theta)^4 \rangle$ further support this average value of μ_θ. The scatter in the data for μ and μ_θ is such that a distinction between magnitudes of μ and μ_θ is not warranted for the present purpose (strictly, the experimental evidence tends to favor a value of μ_θ which is marginally larger than μ). For convenience, we assume here that both μ and μ_θ are equal to 0.25.

In the log-normal model the probability density function of χ_r is assumed, like that of ϵ_r, to be log-normal. The joint probability density of ϵ_r and χ_r is also assumed log-normal and the variance of χ_r, like that of ϵ_r, is proportional to $\ln(l/r)^\mu$. With these assumptions,

$$\langle \epsilon_r^p \chi_r^q \rangle \sim \langle \epsilon \rangle^p \langle \chi \rangle^q \times r^{-\mu[p(p-1)/2+q(q-1)/2+pq\rho]} \ ,$$

where ρ is the correlation coefficient between the centered variables $\ln\epsilon_r$ and $\ln\chi_r$. The structure function $\langle (\Delta\theta)^n \rangle$ is then given by

$$\langle (\Delta\theta)^n \rangle \sim \langle \epsilon \rangle^{-n/6} \langle \chi \rangle^{n/2} \times r^{n/3-\mu n[(10-6\rho)n-12]/72} \ , \tag{11}$$

as originally developed in Ref. 13.

In the β model, statistically stationary turbulence is assumed with energy introduced into the fluid at scales $\sim l$ and then cascaded to smaller and smaller scales. At each step of the cascade, any ith eddy of size $l_i \sim l 2^{-i}$ produces, on the average, I eddies at the $(i+1)$th level. With the largest eddies assumed to be space filling, it is assumed that after i generations only a fraction β_i ($\equiv \beta^i$, where $\beta = I/2^3$) of the space will be occupied by "active" fluid. If we denote by v_i and θ_i typical velocity and temperature differences, respectively, over a distance l_i in an active region, the transfers of energy and temperature variance from ith to $(i+1)$th eddies are given by (5) and (6) if l_i is identified with r. If it is further supposed that a perfect correlation exists between velocity and temperature dissipation fields, the average $\langle (\Delta\theta)^n \rangle$ for the β model follows essentially from Eq. (7). Specifically, $\langle (\Delta\theta)^n \rangle$ will exhibit the same dependence on r as given in Ref. 5, viz.,

$$\langle (\Delta\theta)^n \rangle \sim \langle \epsilon \rangle^{-n/6} \langle \chi \rangle^{n/2} r^{n/3+\mu(3-n)/3} \ . \tag{12}$$

The linear departure from $n/3$ in the exponent ζ_n of r in Eq. (12) contrasts with the quadratic departure in ζ_n for the log-normal model Eq. (11).

The correlation coefficient ρ is not easily accessible experimentally. Available measurements[14,15] have identified ρ with the correlation coefficient between $\ln(\partial u/\partial x)_r^2$ and $\ln(\partial\theta/\partial x)_r^2$. This latter coefficient increases through the inertial range, approximately as $\ln r$. Measurements in Refs. 14 and 15 indicate that an average value for ρ is 0.5. For $\mu = 0.25$ and $\rho = 0.5$, the log-normal model, Eq. (11), predicts a maxium for the exponent ζ_n of r when $n = 8.5$. This suggests that moments of order higher than eight should enable one to decide between the decreasing trend of the log-normal model, Eq. (11), and the increasing trend of the β model Eq. (12).

III. EXPERIMENTAL DETAILS

Measurements were made on the centerline of a turbulent round jet at a distance from the nozzle of 35 nozzle diameters, where the turbulence Reynolds number R_λ is about 850. At this location in the flow, the mean temperature is 5.1 °C above ambient whilst $\langle \theta^2 \rangle^{1/2} \simeq 1.24$ °C and $\langle (\Delta\theta)^2 \rangle^{1/2} \simeq 0.38$ °C when r corresponds to the lower bound of the inertial range. The temperature fluctuation was measured with a 0.63 μm 90%-Pt—10%-Rh cold wire operated with a constant current anemometer; the heating current was chosen equal to 150 μA, so that the signal-to-noise ratio is sufficiently high ($\simeq 3000$) and the contamination by velocity fluctuations is negligible.

The difficulty in obtaining moments for $n > 8$ is illustrated in Fig. 1 which shows $p_{\Delta\theta}$, the probability density function of $\Delta\theta$ for the smallest value of r in the inertial range, taken to be the same as the velocity inertial range defined in Ref. 8. This value of r is chosen here as it

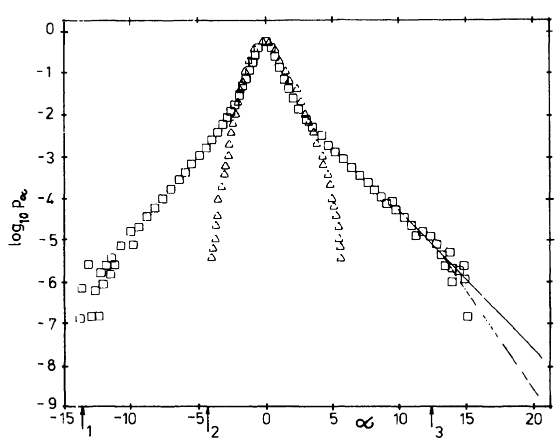

FIG. 1. Probability density functions of θ and $\Delta\theta$ on the axis of a round jet. $x/d = 35$; $R_\lambda \simeq 850$. Δ: p_θ, $\alpha = \theta/\langle \theta^2 \rangle^{1/2}$. $\square$: $p_{\Delta\theta}$, $\alpha = \Delta\theta/\langle (\Delta\theta)^2 \rangle^{1/2}$. 1, $\Delta\theta = -13.4\langle (\Delta\theta)^2 \rangle^{1/2} = \theta_{\min} - \bar{\theta}$; 2, $\theta = -4.1\langle \theta^2 \rangle^{1/2} = \theta_{\min} - \bar{\theta}$; 3, $\theta = +12.4\langle \theta^2 \rangle^{1/2} = \theta_{\max} - \bar{\theta}$. ——, extrapolation assuming exponential behavior for $\alpha \gtrsim 10$; – –, extrapolation obtained by successive approximations of $\alpha^n p_\alpha$ for $n > 8$.

represents the worst case from an experimental point of view, since the tails of $p_{\Delta\theta}$ approach those of the derivative as $r \rightarrow 0$. It is clear from this figure that excursions in $\Delta\theta$ are much larger than for θ whose probability density function is also shown. The negative tail of $p_{\Delta\theta}$ reaches the lower bound of $\Delta\theta$, which corresponds to the difference between the ambient temperature $\theta_{\min}$ and the local mean temperature $\overline{\theta}$. The maximum upper bound of $\Delta\theta$, corresponding to the initial jet temperature level relative to $\theta_{\min}$, is approximately $53\langle(\Delta\theta)^2\rangle^{1/2}$, which is well beyond the range of measured positive or negative excursions. For sufficiently large n, the integrand $(\Delta\theta)^n p_{\Delta\theta}$ does not close and it is necessary to extrapolate $p_{\Delta\theta}$ to achieve closure. One method of extrapolation is to assume that the apparently exponential behavior of $p_{\Delta\theta}$, as indicated by the solid line in Fig. 1, at sufficiently positive $\Delta\theta$ remains unaffected at even larger $\Delta\theta$. A better procedure is to start with $(\Delta\theta)^8 p_{\Delta\theta}$ for which closure is approximately achieved to obtain a closer approximation to $(\Delta\theta)^{10} p_{\Delta\theta}$. The latter integrand is then extrapolated to allow closure of $(\Delta\theta)^{12} p_{\Delta\theta}$. The extrapolation of $p_{\Delta\theta}$ formed using this procedure is also indicated by the dashed line in Fig. 1. Both types of extrapolation were applied to $p_{\Delta\theta}$ obtained at values of r corresponding to the upper and lower bounds, respectively, of the inertial range. Values of ζ_n are shown in Fig. 2, the bounds of the vertical bars corresponding to the two types of extrapolation. It is clear that the uncertainty in determining ζ_n, as represented by the magnitude of the vertical bar, increases with n.

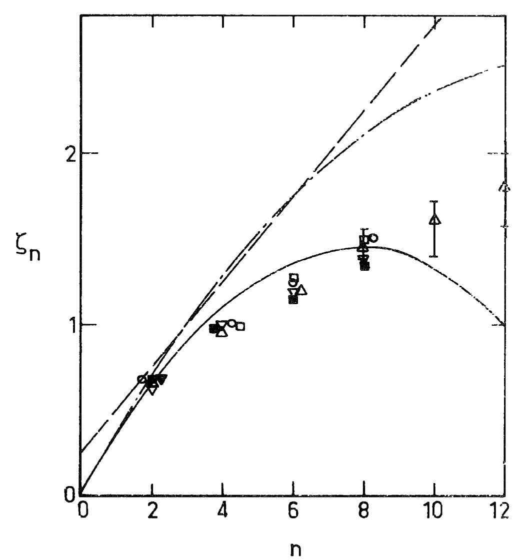

FIG. 2. Inertial-range power-law exponents for temperature structure functions. Experiments: □, atmospheric surface layer over land (Ref. 16); ○, round jet (Ref. 16), ▽, boundary layer (Ref. 17); ■, atmospheric surface layer over ocean (Ref. 15); △, round jet (present study). Models: ——, log-normal, Eq. (11) with $\mu=0.25$, $\rho=0.5$; —·—·, log-normal, Eq. (11) with $\mu=0.25$, $\rho=1$; — —, β, Eq. (12) with $\mu=0.25$.

IV. COMPARISON OF EXPERIMENTS WITH MODELS

The present values of ζ_n for $n \leq 8$ are in good agreement (Fig. 2) with other available measurements obtained in different flows for a wide range of R_λ. The difference between the present value of ζ_{10} and the log-normal model ($\mu=0.25$, $\rho=0.5$) is significantly larger than the experimental uncertainty in determining ζ_{10}. Also, while the log-normal model slightly overestimates the value of ζ_4 and ζ_6, it is a reasonable approximation to the measurements for $n \leq 8$. It is evident, however, that the functional behavior of the log-normal model is inadequate for $n > 8$ and it is also unlikely that refinements in μ and ρ would alter this trend.

The β model with $\mu=0.25$ (and $\rho=1$) predicts values of ζ_n which are increasingly larger, compared with experiment, as n increases. It should be noted, however, that the log-normal model for $\rho=1$ leads to a similar discrepancy between predictions and experiment. It is possible that the introduction in the β model of a nonperfect correlation between velocity and temperature dissipation fields would shift the β-model prediction closer to the experimental data.

It is of interest to compare the exponent ζ_n for temperature with the corresponding exponent α_n for velocity. This comparison is shown in Fig. 3, the experimental values of α_n being those obtained, in the same flow, by Anselmet *et al.*[8] For consistency, a value of 0.25 was retained in presenting Eqs. (2) and (3) in Fig. 3. A value of 0.2 for μ results[8] in a closer agreement, for $n \leq 12$, between experiment and the log-normal model than shown in Fig. 3. In general, the comparison between experimental values of α_n and predictions by Eqs. (2) and (3) reflects that between experimental values of ζ_n and predictions by Eqs. (11) and (12). The differences in the magnitude and rate of increase with n of experimental values of α_n and

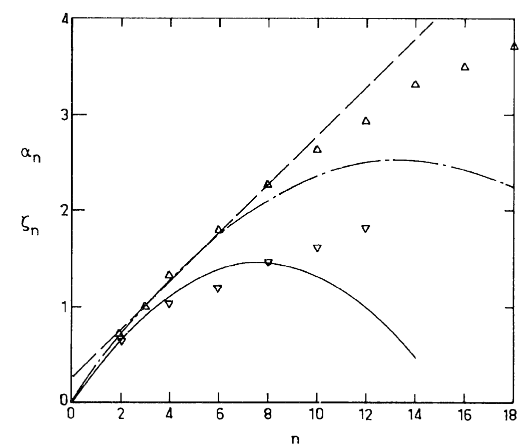

FIG. 3. Comparison of power-law exponents for temperature and velocity structure functions. Experiments: △, α_n (Ref. 8); ▽, ζ_n, present. Models: —·—·, log-normal for α_n, Eq. (2) with $\mu=0.25$; ——, log-normal for ζ_n, Eq. (11) with $\mu=0.25$, $\rho=0.5$; — —, β model for α_n or ζ_n, Eq. (3) or Eq. (12) with $\mu=0.25$.

ζ_n in Fig. 3 together with the sensitivity to ρ of the comparison (Fig. 2) between the log-normal model and experimental values of ζ_n suggest differences between the intermittency of the scalar field and that of the velocity field. This suggestion supports Mori's[11] conjecture that kinetic energy intermittency differs from passive scalar intermittency. Kerr[18] has indicated that the faster rate of increase with the Reynolds number of the flatness factor of $\partial\theta/\partial x$ compared with that of $\partial u/\partial x$ implies that the temperature field is more intermittent than the velocity field. His computer simulations have indicated a strong alignment between the scalar gradient and the rate of strain but little correlation between the magnitudes of the scalar gradient and the vorticity. All of the previous remarks suggest that further investigations of the correlation between scalar and velocity intermittencies, whether they be of an experimental or a computer-simulation nature, should lead to a useful insight into the fine scale structure of turbulence.

ACKNOWLEDGMENTS

R.A.A. gratefully acknowledges the support of the Australian Research Grants Scheme and the generous hospitality of the Institut de Mécanique, Grenoble.

[1]A. N. Kolmogorov, J. Fluid Mech. **13**, 83 (1962).
[2]A. M. Obukhov, J. Fluid Mech. **13**, 77 (1962).
[3]A. M. Yaglom, Dokl. Akad. Nauk SSSR **166**, 49 (1966) [Sov. Phys.—Dokl. **11**, 26 (1966)].
[4]A. S. Monin and A. M. Yaglom, *Statistical Fluid Mechanics* (MIT, Cambridge, Mass., 1975), Vol. 2.
[5]U. Frisch, P-L. Sulem, and M. Nelkin, J. Fluid Mech. **87**, 719 (1978).
[6]E. A. Novikov and R. W. Stewart, Izv. Geophys. **3**, 408 (1964).
[7]R. A. Antonia, B. R. Satyaprakash, and A. K. M. F. Hussain, J. Fluid Mech. **119**, 55 (1982).
[8]F. Anselmet, Y. Gagne, E. Hopfinger, and R. A. Antonia, J. Fluid Mech. **140**, 63 (1984).
[9]M. Nelkin and T. L. Bell, Phys. Rev. A **17**, 363 (1978).
[10]R. A. Antonia, S. Rajagopalan, L. W. B. Browne, and A. J. Chambers, Phys. Fluids **25**, 1156 (1982).
[11]H. Mori, in Proceedings of the IUTAM Symposium on Turbulence and Chaotic Phenomena in Fluids, Kyoto, 1983 (unpublished).
[12]A. J. Chambers and R. A. Antonia, Boundary-Layer Meteorol. **28**, 343 (1984).
[13]C. W. Van Atta, Phys. Fluids **14**, 1803 (1971).
[14]R. A. Antonia and A. J. Chambers, Boundary-Layer Meteorol. **18**, 399 (1980).
[15]J. T. Park, Ph.D. thesis, University of California at San Diego, 1976.
[16]R. A. Antonia and C. W. Van Atta, J. Fluid Mech. **84**, 561 (1978).
[17]P. Mestayer, Thèse Docteur ès Sciences Physiques, Université d'Aix-Marseille II, 1981.
[18]R. M. Kerr, in Proceedings of the Fourth Symposium on Turbulent Shear Flows, Karlsruhe, 1983, edited by C. J. S. Bradbury *et al.* (unpublished).